Supporting Information

Spiro-fluorene Based 3D Donor towards Efficient Organic Photovoltaics

Shuying Ma,[a] Yingying Fu,[b] Debin Ni,[a] Jian Mao,[a]Zhiyuan Xie,[*b] Guoli Tu[*a]

[a] Wuhan National Laboratory for Optoelectronics, Huazhong University of Science and Technology, Wuhan 430074, P. R. China. E-mail: tgl@mail.hust.edu.cn

[b] State Key Laboratory of Polymer Physics and Chemistry, Changchun Institute of Applied Chemistry, Chinese Academy of Sciences, Changchun 130022, P. R. China. E-mail: xiezy_n@ciac.jl.cn

Table of contents:

Experimental Section

Synthetic procedures for compound SF8TBT and LF8TBT

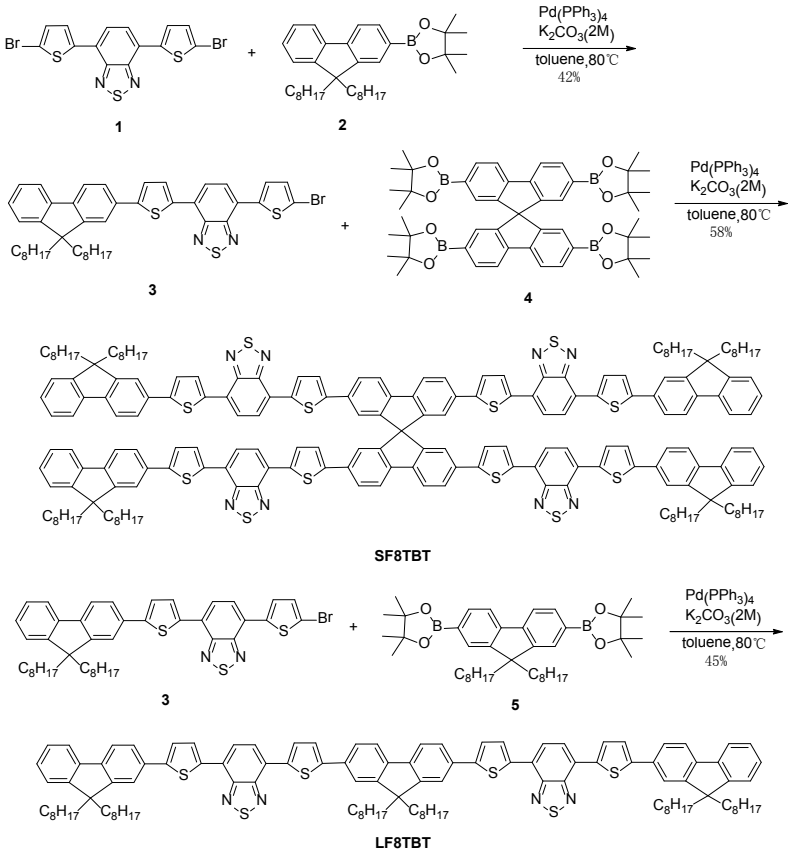

4,7-bis(5-bromothiophen-2-yl)benzo[c][1,2,5]thiadiazole(1), 2-(9,9-dioctyl-9H-fluoren-2-yl)-4,4,5,5-tetramethyl-1,3,2-dioxaborolane (2) and 2,7-Bis(4,4,5,5-tetramethyl-1,3,2-dioxaboronal-2-yl) fluorene (5) were synthesized following the reported method. [1,2,3]

4-(5-bromothiophen-2-yl)-7-(5-(9,9-dioctyl-9H-fluoren-2-yl)thiophen-2-yl)benzo[c][1,2,5]thiadiazole (3): The mixture of **1** (308 mg, 0.60 mmol), **2** (300 mg, 0.66 mmol), tetrakis(triphenylphosphine)palladium(0) (35 mg, 0.03 mmol), 2M aqueous sodium carbonate solution (10 ml) and 20 ml of toluene was heated to 80 ℃ overnight under N_2. The resulting mixture was washed with toluene (20 ml×3) for three times and the organic layers were collected. After washed with brine and dried over Na_2SO_4, the solvent were removed under vacuum to give dark red solid. Then the crude product

was purified by column chromatography (silica, toluene/hexane=1:10) and a dark red solid was obtained (190 mg, 42%). ^{1}HNMR (400 MHz, $CDCl_3$, δ): 8.15 (d, J=3.9 Hz, 1H), 7.91 (d, J=7.6 Hz, 1H), 7.82 (m, 2H), 7.71 (m, 3H), 7.49 (d, J=3.9 Hz, 1H)，7.65 (s, 1H), 7.34 (m, 3H),7.17 (d, J=3.9 Hz, 1 H), 2.02 (m, 4H), 1.26 (m, 24H), 0.80 (t, J=7.1 Hz, 6H).

2,2',7,7'-tetrakis(4,4,5,5-tetramethyl-1,3,2-dioxaborolan-2-yl)-9,9'-spirobi[fluorene] (4): A solution of 2,2',7,7'-tetrabromo-9,9'-spirobi[fluorene] (1.6 g, 2.5 mmol), bis(pinacolato)diboron (3.8 g, 15 mmol), $PdCl_2$(dppf) (0.4 g, 0.5 mmol), and KOAc (2.9 g, 30 mmol) in THF (150 ml) was stirred at 80 ℃ under N_2 for three days. The reaction was quenched by adding water and the resulting mixture was washed ethyl acetate (50 ml×3). Then the organic layers were washed with brine, dried over Na_2SO_4, and concentrated in vacuum. After purified by column chromatography (CH_2Cl_2/hexane), white solid was obtained with yield of 65% (1.35 g). ^{1}HNMR (400 MHz, $CDCl_3$, δ): 7.85 (m, 8H), 7.09 (s, 4H), 1.25 (s, 48H).

SF8TBT: The mixture of **3** (164 mg, 0.2 mmol), **4** (768 mg, 1.0 mmol), tetrakis(triphenylphosphine)palladium(0) (47 mg, 0.04 mmol), 2M aqueous sodium carbonate solution (10 ml) and toluene (20 ml) was heated at 80 ℃ under N_2 for three days. Then the resulting mixture was washed toluene (20 ml×3) and the organic layers were washed with brine, dried over Na_2SO_4. After concentrated under vacuum to remove the solvent, the crude product was purified by column chromatography (toluene/hexane=1:2) to give the desired compound as a dark red solid (360 mg, 58%). High-resolution mass spectrometry (HRMS) (electronionzation (EI)) mass-to-charge

ratio (m/z) : M+ calculated for $C_{197}H_{200}N_8S_{12}$, 3064.53; found 3064.21.

LF8TBT: The mixture of **3** (254 mg, 0.33 mmol), **5** (97 mg, 1.0 mmol), tetrakis(triphenylphosphine)palladium(0) (9 mg, 0.007 mmol), 2M aqueous sodium carbonate solution (10 ml) and toluene (20 ml) was heated to 80 ℃ under N_2 for three days. The reaction was quenched by adding water, and the resulting mixture was washed toluene (20 ml×3). The organic layers were washed with brine, dried over Na_2SO_4, and concentrated in vacuum. After purified by column chromatography (toluene/hexane=1:2), dark red solid was obtained with yield of 45% (120 mg). ^{1}HNMR (400 MHz, $CDCl_3$, δ): 8.16 (m, 4H), 7.94 (s, 4H), 7.71 (m, 15H), 7.51 (m, 4H), 7.35 (m, 6H), 2.06 (m, 12H), 1.25 (m, 72H), 0.80 (t, J=6.9 Hz, 18H). High-resolution mass spectrometry (HRMS) (electronionzation (EI)) mass-to-charge ratio (m/z) : M+ calculated for $C_{115}H_{134}N_4S_6$, 1764.71; found 1764.20.

Copies of ^{1}H NMR Spectra

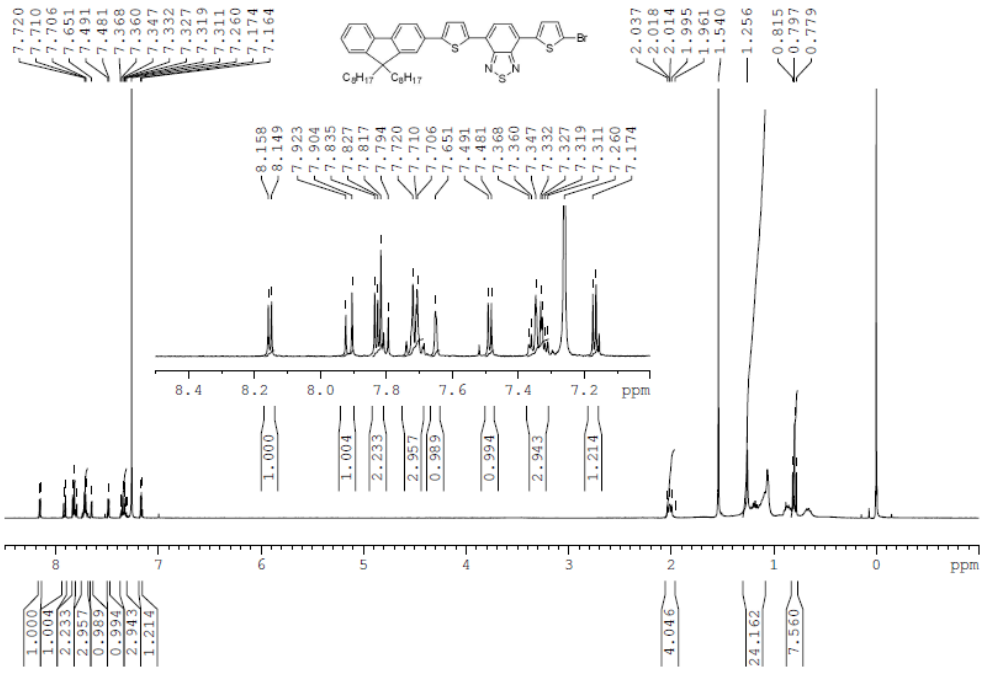

^{1}H NMR spectrum for compound **3**

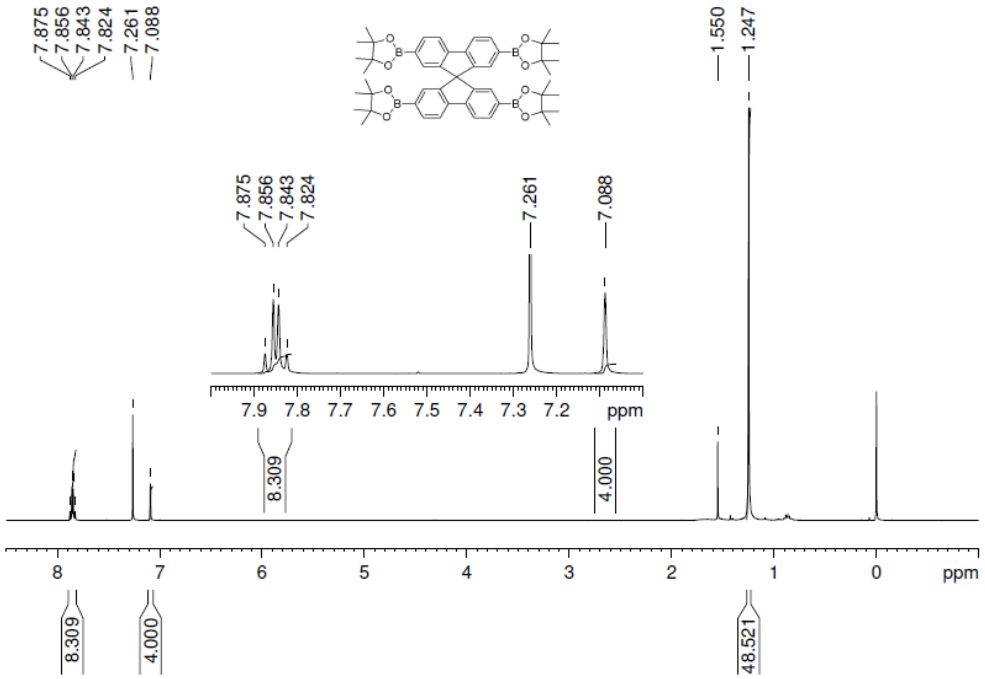

^{1}H NMR spectrum for compound **4**

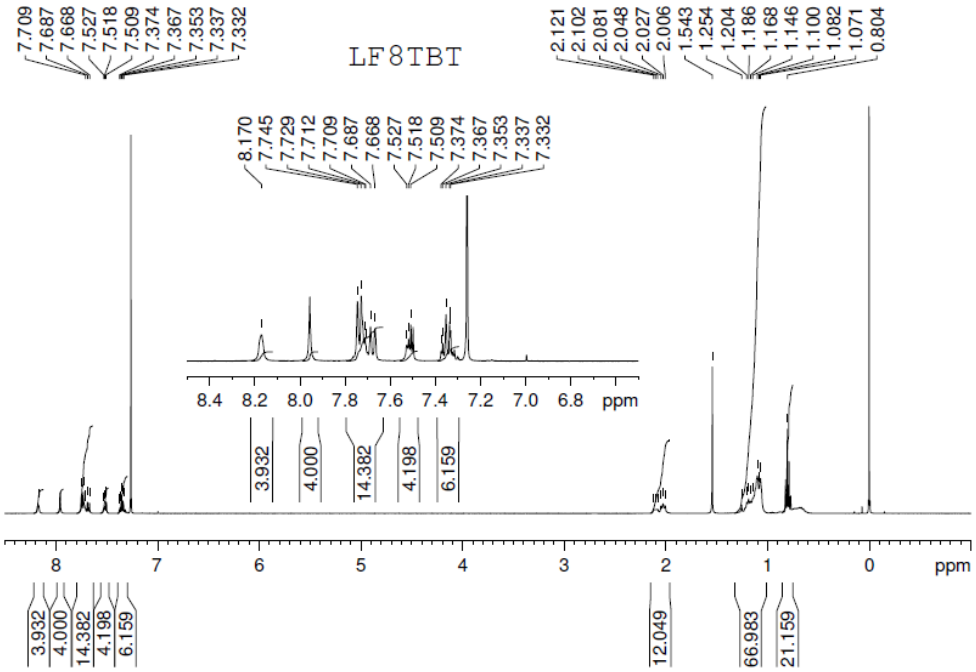

^{1}H NMR spectrum for LF8TBT

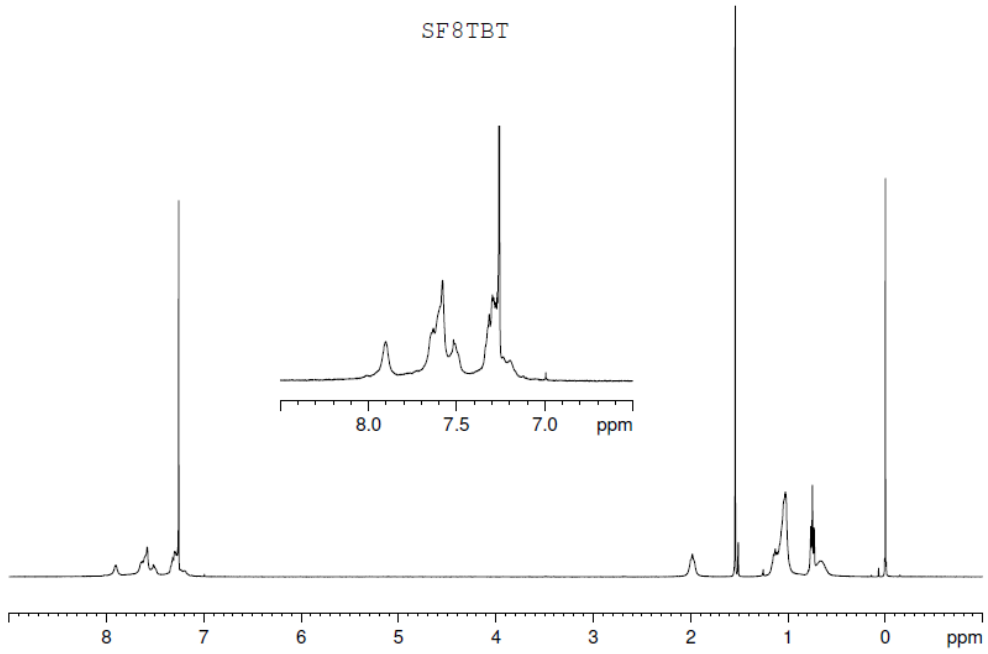

^{1}H NMR spectrum for SF8TBT

X-ray diffraction

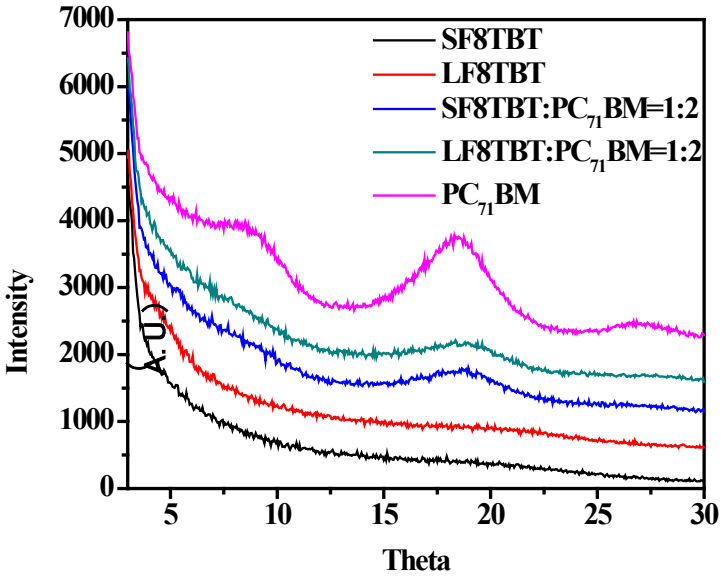

Figure SI 1. XRD data of films of SF8TBT, LF8TBT, SF8TBT:$PC_{71}BM$=1:2, LF8TBT:$PC_{71}BM$=1:2 and $PC_{71}BM$.

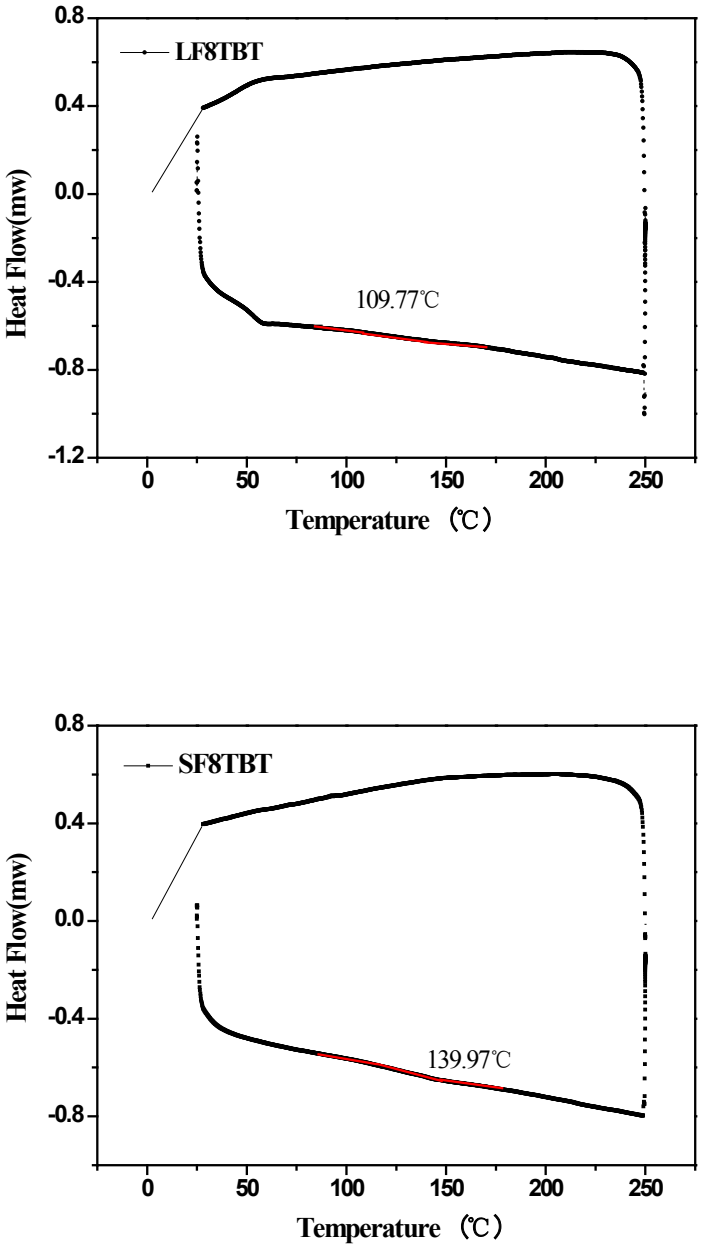

Figure SI 2. Differential scanning calorimetry curves of LF8TBT and SF8TBT. Second cooling and heating curves are shown.

Device fabrication and Characterization: Donor materials (LF8TBT or SF8TBT) were blended with $PC_{71}BM$ in weight ratio of 1:2 in 1,2-dichlorobenzene (DCB) and stirred overnight. The pre-cleaned ITO substrate was treated with UV-ozone for 25 min, and then a 30 nm PEDOT:PSS layer was spin-coated on the ITO substrate from

an aqueous solution (Baytron P VP AI 4083), followed by baking in an oven at 150 °C for 10 min. The active layer was obtained by spin-coating the blend solution at different speed in a glove box without thermal annealing or solvent additives. The active layer thickness was measured with a Dektek profilometer. A bilayer cathode structure of Ca (25 nm)/Al (150 nm) was thermally evaporated atop the active layer in vacuum chamber under a base pressure of about 4×10^{-4} Pa. The cell active area was 0.16 cm^2, which was defined by the overlapping area of the ITO and Al electrodes. An Oriel solar simulator with an AM 1.5G filter was used to provide 100 mW/cm^2 simulated solar light. The light intensity was determined by a calibrated silicon diode with KG-5 filter. The illuminated J-V characteristics of the cells were measured using a computer-controlled Keithley 236 source meter under AM1.5G 100 mW/cm^2 simulated solar light illumination. The IPCE spectra were measured under short-circuit conditions with a lock-in amplifier (SR830, Stanford Research System) at a chopping frequency of 280 Hz during illumination with a monochromatic light from a Xenon lamp. The AFM measurements were performed on SPA300HV instrument with an SPI3800 controller (Seiko Instruments).

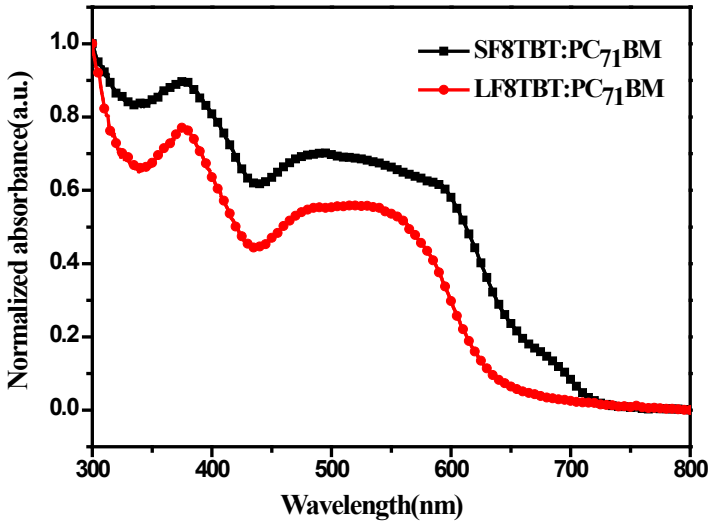

Figure SI 3. Normalized absorption spectrum for the blends SF8TBT:$PC_{71}BM$=1:2 and LF8TBT:$PC_{71}BM$=1:2.

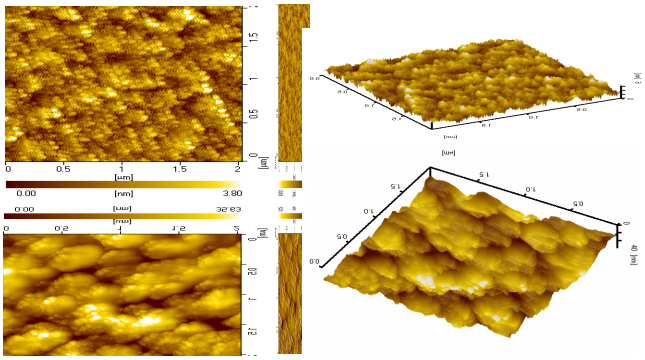

Figure SI 4. AFM topographic images of SF8TBT/$PC_{71}BM$ (top) and LF8TBT/$PC_{71}BM$ (down) in films.

The morphologies of the active layers were obtained by atomic force microscopy

(AFM) by tapping mode, as shown in **Fig. SI 4**. The LF8TBT/$PC_{71}BM$ blend exhibited isolated island structure with large amount of aggregated domains and root-mean-square (RMS) roughness of 6.45 nm (Fig. 2, bottom). The domain sizes were estimated by cross-section profiles to be about 100 nm, much larger than the efficient exciton diffusion distance. Different to the morphology of LF8TBT/$PC_{71}BM$ blend, the AFM images of SF8TBT/$PC_{71}BM$ blend (105 nm, Fig. 2, top) showed a RMS of 0.91 nm and smaller domain with size about 30 nm, exhibiting a good miscibility with $PC_{71}BM$ molecules in the blend films and optimized donor/acceptor interpenetrating network. The AFM images of SF8TBT/$PC_{71}BM$ blend showed no dependence to the thickness and the 65 nm film exhibited almost the same morphology as that of 105 nm. The above comparison of AFM results indicates that, compared with the liner small molecules, the 3D spiro molecules of donor materials can be used to control the morphologies in the active layers, leading to efficient exciton separation and higher FF, combining with higher J_{sc} due to the application of thicker films.

References:

[ ] X. Zhang, R. Yamaguchi, K. Moriyama, M. Kadowaki, T. Kobayashi, T. Ishi-i, T. Thiemanna, S. Mataka, *J. Mater. Chem.* **2006**, *16*, 736.

[2] P. Anant, N. T. Lucas, J. Jacob, *Org. Lett.* **2008**, *10*, 24.

[3] S. J. Liu, Q. Zhao, R. F. Chen, Y. D, Q. L. F, F. Y. L, L. H. Wang, C. H. H, W. Huang, *Chem. Eur. J.* **2006**, *12*, 4351.